

## Thermodynamic Stability of Boron: The Role of Defects and Zero Point Motion

Michiel J. van Setten,<sup>†</sup> Matthé A. Uijtewaal,<sup>†</sup> Gilles A. de Wijs,<sup>\*,†</sup>  
and Robert A. de Groot<sup>†,‡</sup>

*Contribution from the Electronic Structure of Materials, Institute for Molecules and Materials, Faculty of Science, Radboud University Nijmegen, Toernooiveld 1, 6525 ED Nijmegen, The Netherlands, and Solid State Chemistry Laboratory, MSC, University of Groningen, Nijenborgh 4, 9747 AG Groningen, The Netherlands*

Received May 4, 2006; E-mail: G.deWijs@science.ru.nl

**Abstract:** Its low weight, high melting point, and large degree of hardness make elemental boron a technologically interesting material. The large number of allotropes, mostly containing over a hundred atoms in the unit cell, and their difficult characterization challenge both experimentalists and theoreticians. Even the ground state of this element is still under discussion. For over 30 years, scientists have attempted to determine the relative stability of  $\alpha$ - and  $\beta$ -rhombohedral boron. We use density functional calculations in the generalized gradient approximation to study a broad range of possible  $\beta$ -rhombohedral structures containing interstitial atoms and partially occupied sites within a 105 atoms framework. The two most stable structures are practically degenerate in energy and semiconducting. One contains the experimental 320 atoms in the hexagonal unit cell, and the other contains 106 atoms in the triclinic unit cell. When populated with the experimental 320 electrons, the 106 atom structure exhibits a band gap of 1.4 eV and an in-gap hole trap at 0.35 eV above the valence band, consistent with known experiments. The total energy of these two structures is 23 meV/B lower than the original 105 atom framework, but it is still 1 meV/B above the  $\alpha$  phase. Adding zero point energies finally makes the  $\beta$  phase the ground state of elemental boron by 3 meV/B. At finite temperatures, the difference becomes even larger.

### 1. Introduction

The element boron has exceptional properties such as a low volatility and a high melting point (2450 °C); it is stronger than steel, harder than corundum, and lighter than aluminum.<sup>1</sup> Moreover, boron has a small reactivity at room temperature. It is under investigation as a constituent in hydrogen storage materials (e.g., LiBH<sub>4</sub>),<sup>2</sup> and it is used in high power electronics (LaB<sub>6</sub>),<sup>3</sup> in superconductors (MgB<sub>2</sub>,  $T_C = 39$  K),<sup>4</sup> in heat-resistant alloys, as wall coatings in nuclear reactors, and as dopant in or alternatives to carbon systems (nanotubes, polymers, diamond, graphite).

Even though there is a wide interest in boron, the element is far from completely understood. As many as 16 boron allotropes are known. The cubic form is only known to encompass 1708 atoms in the unit cell, and the 192 atom tetragonal and the 12 atom  $\alpha$ -rhombohedral (AR) crystal structures are the only ones that are well characterized.

However, the most stable polymorph, at least at high temperatures, is the  $\beta$ -rhombohedral (BR) structure.<sup>5</sup> In 1970,

a framework consisting of 105 atoms was proposed.<sup>6</sup> Later, in 1988, it was shown experimentally that the unit cell contains 320 valence electrons, where the electron count was corrected by interstitial atoms and partial occupations.<sup>7,8</sup> At the same time, BR boron was found to be a semiconductor with a band gap of 1.6 eV.

Various theoretical papers were dedicated to finding the BR structure. The first calculations on the BR 105 atom framework were performed by Bullett<sup>9</sup> in 1982. He discusses the electronic structure of AR and BR boron in terms of icosahedra, the building blocks of both structures. Both structures are an attempt of nature to reconcile the 5-fold symmetry of the perfect icosahedra with a space filling crystal structure. In 2001, Jemmis et al.<sup>10,11</sup> analyzed the bonding in the 105 atom framework by a cluster fragment approach. They divided the structure into B<sub>57</sub> and B<sub>12</sub> units and used their recent *nmo* rule to show that the former have electron excess, whereas the latter are electron-deficient. The net count provides a rationalization of the electron

<sup>†</sup> Radboud University Nijmegen.

<sup>‡</sup> University of Groningen.

(1) Sullenger, D. B.; Kennard, C. H. L. *Sci. Am.* **1966**, *215*, 96–107.

(2) Schlapbach, L.; Züttel, A. *Nature* **2001**, *414*, 353–358.

(3) Zhang, H.; Zhang, Q.; Tang, I.; Qin, L. C. *J. Am. Chem. Soc.* **2005**, *127*, 2862–2863.

(4) Nagamatsu, J.; Nakagawa, N.; Muranaka, T.; Zenitani, Y.; Akimitsu, J. *Nature* **2001**, *410*, 63–64.

(5) Hoard, J. L.; Newkirk, A. E. *J. Am. Chem. Soc.* **1960**, *82*, 70–76.

(6) Hoard, J. L.; Sullenger, D. B.; Kennard, C. H. L.; Hughes, R. E. *J. Solid State Chem.* **1970**, *1*, 268–277.

(7) Slack, G. A.; Hejna, C. I.; Garbaskas, M. F.; Kasper, J. S. *J. Solid State Chem.* **1988**, *76*, 52–63.

(8) Slack, G. A.; Hejna, C. I.; Garbaskas, M.; Kasper, J. S. *J. Solid State Chem.* **1988**, *76*, 64–86.

(9) Bullett, D. W. *J. Phys. C: Solid State Phys.* **1982**, *15*, 415–426.

(10) Jemmis, E. D.; Balakrishnarajan, M. M. *J. Am. Chem. Soc.* **2001**, *123*, 4324–4330.

(11) Jemmis, E. D.; Balakrishnarajan, M. M.; Pancharatna, P. D. *J. Am. Chem. Soc.* **2001**, *123*, 4313–4323.

**Table 1.** Optimized Crystal Structure of  $\alpha$ -Boron, Space Group  $R\bar{3}m$  (No. 166), Compared to the Experimental Structure<sup>30</sup>

cell parameters	<i>a</i>	<i>c</i>	volume
this work	4.9027	12.5367	260.97
exp	4.9179	12.5805	263.50
	Wyckoff positions	<i>x</i>	<i>z</i>
exp	B1 18h	0.1189	0.8913
this work		0.1185	0.8914
exp	B2 18h	0.1969	0.0243
this work		0.1963	0.0241

**Table 2.** Partial Occupation (Number of Atoms) of Sites of BR Boron According to Slack et al.<sup>7</sup> for the Three Samples Reported (A, B, and C)

site	Wyckoff position	A	B	C
B13	18h	14.0	13.4	13.1
B16	18h	4.6	4.9	5.1
B17	18h	1.2	1.5	1.7
B18	18h	1.0	1.2	1.3
B19	18h	1.3	1.2	1.3
B20	36h	0.0	1.3	0.9
total		22.1	23.5	23.4

deficiency of BR boron that was already pointed out by Bullett. Next, in 2002, Imai et al.<sup>12</sup> considered, using density functional theory (DFT) in the local density approximation (LDA), a single atom substitution which increased the stability. In 2005, Prasad et al.<sup>13</sup> concluded from DFT/LDA calculations that AR boron is more stable than the BR 105 atom framework. Finally, in a very recent paper by Masago et al.,<sup>14</sup> a DFT/LDA study is reported in which more systematic single atom replacements were made in the 105 atom framework. Furthermore, they calculated  $\Gamma$ -phonon modes to investigate the temperature dependence of the relative stability of AR boron and the 105 atom framework of BR boron. They concluded that above 1400 K the latter is thermodynamically more stable. However, no BR structure with the right number of electrons has yet been calculated. Moreover, no calculation produced a gap in the electronic density of states (DOS). Neither is it clear that BR boron then provides the ground state structure.

In this paper, we investigate the ground state structure of boron by means of ab initio calculations. We study various atomic substitutions in and extensions to the 105 atom BR framework and develop general rules to guide us to the ground state structure. Total energies and electronic DOS are also calculated for AR boron. Finally, we investigate how phonons, both in the zero point energy (ZPE) and at finite temperatures, determine the relative stability of the BR and the AR structure.

The paper is organized as follows. First we give the details of the computational methods used. Then we discuss the AR boron structure. The next section is dedicated to the various BR structures. Then the AR and BR structures are compared, and finally we state the main conclusions.

## 2. Computational Methods

First-principles calculations were performed within DFT,<sup>15</sup> using the Perdew–Wang '91 generalized gradient approximation (GGA) func-

- (12) Imai, Y.; Mukaida, M.; Ueda, M.; Watanabe, A. *J. Alloys Compd.* **2002**, *347*, 244–251.  
 (13) Prasad, D. L. V. K.; Balakrishnarajan, M. M.; Jemmis, E. D. *Phys. Rev. B* **2005**, *72*, 195102-1–6.  
 (14) Masago, A.; Shirai, K.; Katayama-Yoshida, H. *Phys. Rev. B* **2006**, *73*, 104102-1–10.  
 (15) Kohn, W. *Rev. Mod. Phys.* **1999**, *71*, 1253–1266.

**Table 3.** Total Energies (meV/B Relative to the BR 105 Structure) and Description of All Calculated Structures of BR Boron, Indicating the Vacant B13 and the Filled B16–20B Sites (The Nomenclature Introduced in the Text is Used to Describe the Unit Cell)

system	-B13			+B16			B17	B18	B19	B20	<i>E</i>
	slab	1	2	3	1	2					
105	—	—	—	—	—	—	—	—	—	—	0
111	—	—	—	all	all	all	—	—	—	—	100
105B16	<i>a</i>	<i>a</i>	<i>a</i>	<i>a</i>	<i>a</i>	<i>a</i>	—	—	—	—	-10
106B16a	<i>a</i>	<i>a</i>	<i>a</i>	$\bar{a}\bar{a}$	$\bar{a}\bar{a}$	$\bar{a}\bar{a}$	—	—	—	—	-18
106B16b	<i>a</i>	<i>a</i>	<i>a</i>	$\bar{a}\bar{b}$	$\bar{a}\bar{b}$	$\bar{a}\bar{b}$	—	—	—	—	-23
106B19	<i>a</i>	<i>a</i>	<i>a</i>	$\bar{b}$	$\bar{b}$	$\bar{b}$	—	—	123 <i>a</i>	—	-21
320EXP	<i>a</i>	<i>a</i>	<i>bc</i>	$\bar{a}\bar{b}$	$\bar{b}$	$\bar{a}\bar{b}$	3 <i>a</i>	3 <i>a</i>	2 <i>a</i>	2 <i>c</i>	-17
320B16	<i>a</i>	<i>a</i>	<i>a</i>	$\bar{c}\bar{b}$	$\bar{c}\bar{b}$	$\bar{a}\bar{b}$	—	—	12 <i>a</i>	—	-22
320B19	<i>a</i>	<i>a</i>	<i>a</i>	$\bar{c}\bar{b}$	$\bar{c}\bar{b}$	$\bar{b}$	—	—	123 <i>a</i>	—	-23

tional.<sup>16</sup> In our opinion, a GGA is preferable over standard LDA, as GGAs correct for many of the deficiencies of LDA, such as the well-known over-binding. The projector augmented wave (PAW) method<sup>17,18</sup> was used as implemented in the total energy and molecular dynamics Vienna Ab initio Simulation Package (VASP).<sup>19–22</sup> Nonlinear core corrections were applied.<sup>23</sup>

The Kohn–Sham orbitals were expanded in plane waves with kinetic energy cutoffs of 400 eV (the total energy differences listed in Table 3 were calculated with this cutoff). We checked basis set completeness by calculating the total energy difference between AR and BR boron both with 400 and 700 eV cutoff. Changing the cutoff affected the total energy difference by merely 0.03 meV/atom (the total energies finally compared were recalculated using the 700 eV kinetic energy cutoff).

The Brillouin zones were sampled with  $10 \times 10 \times 10$  (12 AR),  $4 \times 4 \times 4$  (105 and 111 BR),  $3 \times 3 \times 3$  (106 BR), and  $3 \times 3 \times 1$  (320 BR) Monkhorst–Pack *k*-point grids,<sup>24</sup> resulting in 110, 13, 14, and 5 *k*-points, respectively, in the irreducible parts. The Brillouin zone integration was performed with a modified tetrahedron method.<sup>25</sup>

The calculated total energy differences between the boron phases and the  $\beta$ -rhombohedral structures are on the order of several millielectronvolts per atom. Such energy differences may seem small, and one might wonder whether they can be calculated reliably (with a method such as the PAW method). However, they are calculated as energy differences between cells that contain many atoms and are structurally similar. For example, we obtain energy differences of several millielectronvolts/atom when moving one boron atom from one site to another site within an otherwise unaffected cell (save for relaxation in response to the moving atom) of approximately a hundred atoms (see Table 3). The actual energy change for the displacement of this single atom is 2 orders of magnitude larger. Following similar reasoning, the small energy differences between the  $\alpha$ - and  $\beta$ -rhombohedral structures can also be reliably calculated, as both phases have many structural similarities, both being based on the icosahedron as a basic building block. Very high accuracies have even been obtained with (more-approximate) pseudopotential methods, such as in the free energy difference between  $\alpha$ - and  $\beta$ -Sn.<sup>26</sup>

- (16) Perdew, J. P.; Chevary, J. A.; Vosko, S. H.; Jackson, K. A.; Pederson, M. R.; Singh, D. J.; Fiolhais, C. *Phys. Rev. B* **1992**, *46*, 6671–6687.  
 (17) Kresse, G.; Joubert, D. *Phys. Rev. B* **1999**, *59*, 1758–1775.  
 (18) Blöchl, P. E. *Phys. Rev. B* **1994**, *50*, 17953–17979.  
 (19) Kresse, G.; Furthmüller, J. *Phys. Rev. B* **1996**, *54*, 11169–11186.  
 (20) Kresse, G.; Furthmüller, J. *Comput. Mater. Sci.* **1996**, *6*, 15–50.  
 (21) Kresse, G.; Hafner, J. *Phys. Rev. B* **1993**, *47*, 558–561.  
 (22) Kresse, G.; Hafner, J. *Phys. Rev. B* **1994**, *49*, 14251–14269.  
 (23) Louie, S.; Froyen, S.; Cohen, M. *Phys. Rev. B* **1982**, *26*, 1738–1742.  
 (24) Monkhorst, H. J.; Pack, J. D. *Phys. Rev. B* **1976**, *13*, 5188–5192.  
 (25) Blöchl, P. E.; Jepsen, O.; Anderson, O. *Phys. Rev. B* **1994**, *49*, 16223–16233.  
 (26) Pavone, P.; Baroni, S.; de Gironcoli, S. *Phys. Rev. B* **1998**, *57*, 10421–10423.

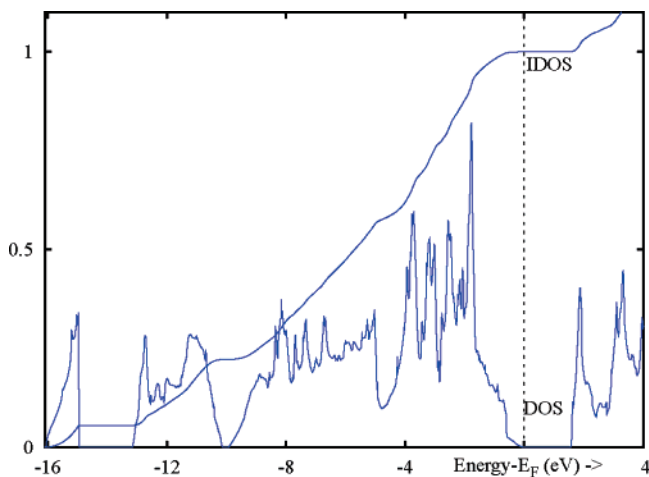


**Figure 1.** Electronic DOS (states/eV/B), energy relative to  $E_F$ , of AR boron. Integrated DOS (IDOS) (number of electrons/36) is also plotted.

Phonon frequencies were calculated using a finite difference method.<sup>27</sup> Displacements of 5 mÅ and supercells of  $2 \times 2 \times 2$  primitive cells for AR boron and the primitive cell for BR boron were found to give frequencies numerically converged to within  $1 \text{ cm}^{-1}$ . From the phonon modes, we calculated the ZPEs and temperature-dependent crystal free energies in the full Brillouin zone. The ZPEs are estimated to be converged to within 0.1 meV/B.

### 3. $\alpha$ -Rhombohedral Boron

The crystal structure, bonding, and lattice dynamics of AR boron are well understood and described extensively in the literature, (e.g., Bullett<sup>9</sup> or Vast et al.<sup>28,29</sup> and references therein). However, we need a very accurate total energy for AR boron to determine whether AR or BR boron is most stable. We therefore performed a relaxation of all atomic and cell parameters and calculated the total energy and electronic DOS. Table 1 shows that both the lattice parameters and atomic positions of the fully relaxed cell agree with the experimental values to a degree that is usual for DFT calculations.

The total energy of the experimental cell with relaxed atomic positions is  $-6.6879 \text{ eV}$  per boron atom (eV/B). Relaxing the cell parameters as well lowers the total energy by only 0.2 meV/B to  $-6.6881 \text{ eV/B}$ . The energies are relative to those of non-spin-polarized atoms. The calculated packing fraction in this cell is 41% (the packing fractions are calculated using a radius of 0.89 Å for the boron atoms). The calculated bulk modulus is 208 GPa, where the experimental values range from 213 to 224 GPa.<sup>31</sup> Previously calculated bulk moduli range from 222 to 260 GPa.<sup>32–34</sup>

In Figure 1, the calculated electronic DOS of AR boron is shown. AR boron has an indirect band gap of 1.54 eV and a direct band gap of 1.94 eV. Dipole-allowed optical transitions have an onset at 2.59 eV. Previous calculations produced indirect

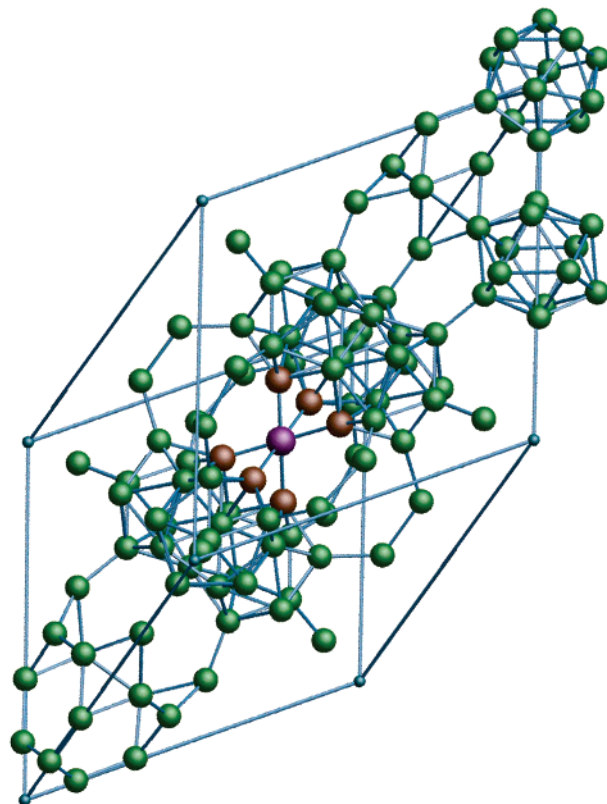


**Figure 2.** Side view of the unit cell of 105 atom BR boron. Most atoms are part of icosahedra. The central atom (purple) is in the B15 position and connects the two groups of three interpenetrating icosahedra via atoms at B13 sites (red).

band gaps of 1.4–1.7 eV<sup>9,33,35,36</sup> and direct gaps from 1.8 to 2.3 eV.<sup>9,33,36</sup> On the basis of optical experiments, Horn suggests a (direct) gap of approximately 2.0 eV.<sup>37</sup> Terauchi et al.<sup>38</sup> derived a (direct) optical gap of 2.4 eV from their electron energy loss experiment. In general, the calculated results are in reasonable agreement with experiments.

### 4. $\beta$ -Rhombohedral Boron

#### 4.1. 105 Atom Framework and B16 Interstitial Position.

The 105 atom framework for BR boron that was proposed by Hoard<sup>6</sup> is very open and consists of 15 nonequivalent boron positions (B1 up to B15). It is well described in the literature (e.g., Jemmis et al.<sup>10</sup>) and shown in Figure 2. We only mention here that the single B15 atom, at the center, connects two B<sub>28</sub> fragments by bonding to the six atoms at B13 sites. This framework is the starting point for further study. The BR structure has space group  $R\bar{3}m$  (No. 166) with lattice constants  $a = 10.139 \text{ Å}$  and  $\alpha = 65.2^\circ$ .<sup>6</sup> These values were used for all BR structure calculations up to the point where the AR and BR structures are finally compared. Of course in all those calculations the atomic positions were optimized.

The calculated electronic DOS of this structure is plotted in Figure 3. There is an energy gap of 1.13 eV at an electron count of 320, whereas the structure itself holds 315 electrons. The

(27) Kresse, G.; Furthmüller, J.; Hafner, J. *Europhys. Lett.* **1995**, *32*, 729–734.

(28) Vast, N.; Baroni, S.; Zerah, G.; Besson, J. M.; Polian, A.; Grimsditch, M.; Chervin, J. C. *Phys. Status Solidi B: Basic Res.* **1996**, *198*, 115–119.

(29) Vast, N.; Baroni, S.; Zerah, G.; Besson, J. M.; Polian, A.; Grimsditch, M.; Chervin, J. C. *Phys. Rev. Lett.* **1997**, *78*, 693–696.

(30) Will, G.; Kiefer, B. *Z. Anorg. Allg. Chem.* **2001**, *627*, 2100–2104.

(31) Nelmes, R. J.; Loveday, J. S.; Allan, D. R.; Besson, J. M.; Hamel, G.; Grima, P.; Hull, S. *Phys. Rev. B* **1993**, *47*, 7668–7673.

(32) Vast, N.; Besson, J. M.; Baroni, S.; Dal Corso, A. *Comput. Mater. Sci.* **2000**, *17*, 127–132.

(33) Li, D.; Xu, Y. N.; Ching, W. Y. *Phys. Rev. B* **1992**, *45*, 5895–5905.

(34) Mailhot, C.; Grant, J. B.; McMahan, A. K. *Phys. Rev. B* **1990**, *45*, 9033–9039.

(35) Häussermann, U.; Simak, S. I.; Ahuja, R.; Johansson, B. *Phys. Rev. Lett.* **2003**, *90*, 065701-1–4.

(36) Bylander, D. M.; Kleinmann, L.; Lee, S. *Phys. Rev. B* **1990**, *42*, 1394–1403.

(37) Horn, F. H. *J. Appl. Phys.* **1959**, *30*, 1611–1612.

(38) Terauchi, M.; Kawamata, Y.; Tanaka, M.; Takeda, M.; Kimura, K. *J. Solid State Chem.* **1997**, *133*, 156–159.

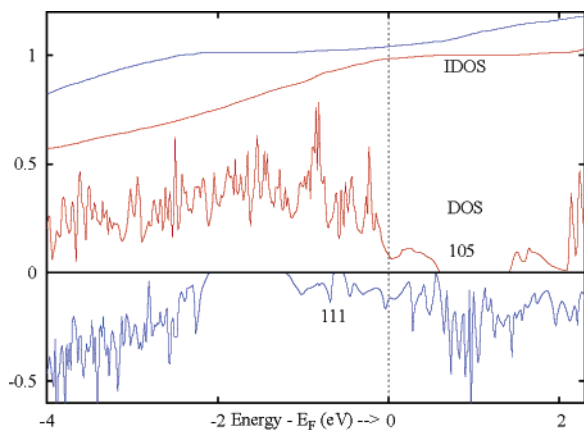


**Figure 3.** Electronic DOS (states/eV/B), energy relative to  $E_F$ , of 105 and 111 atom BR boron. Integrated DOS (number of electrons/320) are also plotted. The energy gaps are at an electron count of 320.

DOS compares well with the calculated band structure by Prasad et al.,<sup>13</sup> which has a gap of 1.03 eV. In their calculation, however, the 105 atom BR structure is 280 meV/B less stable than the AR structure while we only find a difference of 26 meV/B. We do not understand this large discrepancy. Häussermann et al.<sup>35</sup> found an energy difference of 20 meV/B, which agrees well with our value. Nevertheless, BR boron is known to be a semiconductor. This indicates that additional atoms are required.

The BR structure was experimentally refined by Callmer et al.<sup>39</sup> They found one additional boron position (B16) that was fully occupied and so obtained a unit cell of 111 atoms. After structural relaxation, we find that this structure is 100 meV/B less stable than the 105 atom framework. The DOS of the refined structure is also shown in Figure 3. The energy gap is now 0.84 eV and is positioned *below*  $E_F$ .

**4.2. Partial Occupations.** Further experimental refinement of the BR boron structure by Slack<sup>7</sup> showed that the (hexagonal) unit cell contains 320 atoms with lattice constants  $a = 10.93 \text{ \AA}$  and  $c = 2.178a$ . This results in a density of  $2.333 \text{ g/cm}^3$  and a packing fraction of only 38%, which is lower than the value for AR boron. The atoms are distributed over four additional sites (B17 up to B20), and the previously mentioned B13 and B16 positions are also partially occupied. The atomic occupation numbers of the B13 and B16–B20 sites for the three samples reported are given in Table 2.

Jemmis et al.<sup>10</sup> analyzed the bonding in the 105 atom framework by means of electronic structure calculations in the molecular fragments approach. They find that three B13 sites must be vacant and eight boron atoms should be distributed over B16, B19, and B20 sites to saturate all bonds in the hexagonal unit cell. The B16, B19, and B20 sites are placed around the so-called “A” hole in the framework and form tetrahedra. These tetrahedra are connected in triples by means of the atoms at the B16 sites.

The B13, B16, and B19 positions are depicted in Figure 4. The left panel shows that the partially occupied sites are located in three equivalent slabs in the hexagonal unit cell. Each B17 site (not shown for clarity) is located very close to two B13 sites and is somewhat displaced toward the middle of the slab.

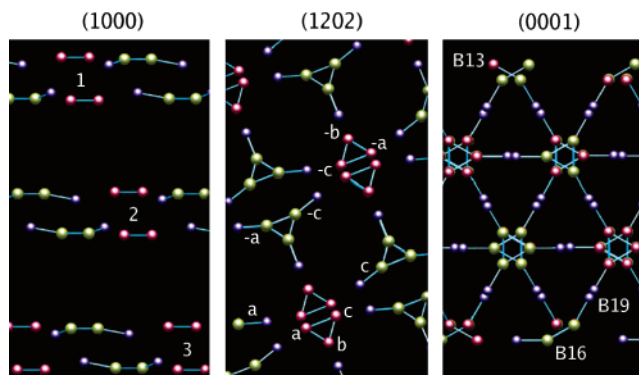


**Figure 4.** The most important partial occupied sites of BR boron in the hexagonal cell, seen along the (1000) vector (left), along the (1202) vector (middle), and along the (0001) vector (right). B13 atoms are indicated in red, B16s in yellow, and B19 positions in dark blue. The numbering scheme introduced in the text is indicated. It makes the atoms individually addressable.

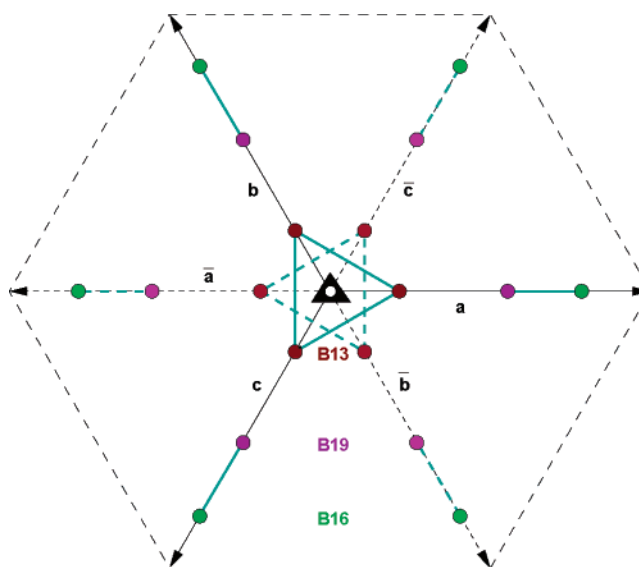


**Figure 5.** Naming scheme for the B13, B16, and B19 sites in one slab in the hexagonal cell.

The atoms at the B18 sites bond to atoms at B17 sites and are located very close to the B19 sites on the other side of the slab. We introduce a numbering scheme to be able to address all atoms individually. The three slabs are numbered 1–3. Within each slab, there is a  $\bar{3}$  axis, as schematically illustrated in Figure 5. Starting from a triple of B13 sites, we call the three directions in the slab  $a$ ,  $b$ , and  $c$ . The other three (point symmetric) B13 sites are then positioned in the  $\bar{a}$ ,  $\bar{b}$ , and  $\bar{c}$  direction. The same nomenclature applies to all the B16 up to B20 sites as they are all placed within the slabs and according to the same 3-fold axis. For example, the B16 site that lies along the same vector as the  $3\bar{a}$  B13 site (3 is the slab number) is the  $3\bar{a}$  B16 site and the B17 site connecting both  $2a$  and  $2b$  B13 sites is the  $2\bar{c}$  B17 site. Except for a pair of B20 sites, every site has a unique designation.

In the following, we will consider several structures in unit cells containing up to 320 atoms that are approximations to the experimental ground state structures. The (free) energies of those structures provide an upper bound to those of the experimental structures.

(39) Callmer, B. *Acta Crystallogr. Sect. B: Struct. Commun.* **1977**, *33*, 1951–1954.

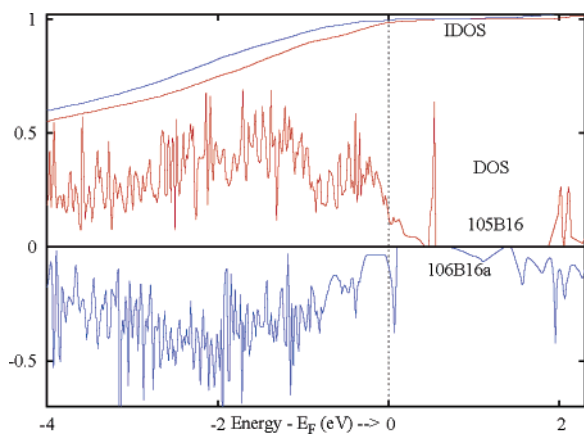


**Figure 6.** Electronic DOS (states/eV/B), energy relative to  $E_F$ , of 105B16 (blue, lower graph) and 106B16a (red, upper graph) atom BR boron. The  $aB13$  atom is removed, and the  $aB16$  and the  $\pm aB16$  atoms are added, respectively. The Fermi levels are indicated with vertical lines, and the IDOS (number of electrons/320) is also plotted.

The first step to the ground state structure is to consider single atom substitutions in the 105 atom framework. Theory<sup>10</sup> and experiments (see Table 2) agree that at least one B13 site is vacant and one atom should be added at a B16 site. This is precisely what was done by Imai et al.,<sup>12</sup> but it was not mentioned at which B16 site the boron was added. Furthermore, no structural relaxation was included. The energy decreased by no less than 20 meV/B, but they indicate that their kinetic energy cutoff was not large enough to have reached convergence. The DOS from these calculations has a large band gap of 1.3 eV above  $E_F$ . This gap is reproduced (1.4 eV) in our DOS, as shown in Figure 6. In our structure (labeled 105B16, see Table 3), the atom at the  $aB13$  site is moved to the (nearest)  $aB16$  site. This decreases the energy by 10 meV/B. Recently, Masago et al.<sup>14</sup> also calculated the effect of B13–B16 swaps, considering all B16 sites possible within the 105 atom unit cell. They find that the energy decreases by 4 meV/B. We attribute this difference to the different exchange–correlation functionals used; Masago et al. used plain LDA, whereas we employ the Perdew–Wang ’91 GGA.<sup>16</sup>

Motivated by symmetry considerations, we subsequently added an atom at the  $\bar{a}B16$  site (106B16a). The energy lowers by another 8 meV/B. The gap in the DOS, at an electron count of 320, has decreased quite somewhat to 0.65 eV (Figure 6). However, these structures are still electron-deficient. Imai et al.<sup>12</sup> also considered a 106 atom structure, where they occupied a B17 site. It resulted in a raising of the total energy per atom compared to the 105 atom framework, which is presumably due to not having carried out a structural relaxation.

Next, total energy calculations were done in the (three times as large) hexagonal 320 atom unit cell. We considered three vacant B13 sites and various distributions of the eight interstitial atoms. We conclude the following from these calculations: (1) A B17 site can only be occupied when two neighboring B13 sites are vacant. (2) Simultaneously, the neighboring B18 sites must be filled. (3) A B16 and B19 boron should not neighbor an occupied B17 site. (4) It is, in fact, favorable to leave the B17 and B18 positions vacant altogether. (5) At each side of a slab, at least one B16, B19, or B20 site should be occupied. (6) No neighboring B16, B19, and B20 sites should be filled simultaneously. (7) The opposite interstitial sites (e.g.,  $a$  and

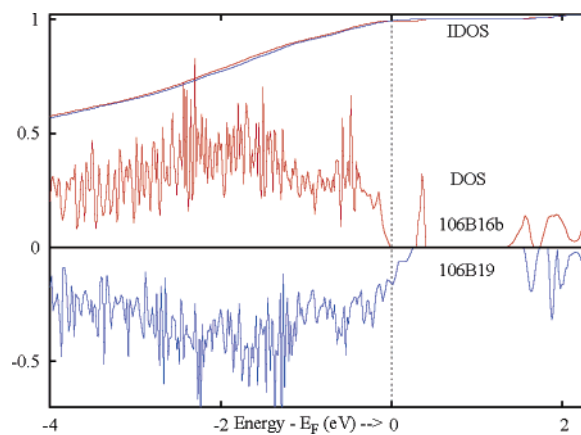


**Figure 7.** Electronic DOS (states/eV/B), energy relative to  $E_F$ , of 106 atom BR boron. Integrated DOS (number of electrons/320) is also plotted. The  $aB13$  atom is replaced by the  $\bar{b}B16$  boron and, respectively, the  $aB16$  (106B16b) (red, upper graph) and the 106B19 (blue, lower graph) boron.

$\bar{a}$ ) in one slab should not be occupied simultaneously. (8) A filled B19 site is slightly more stable than a B20 site. (9) The filled B16 sites are more stable than the B19 interstitial sites. (10) When a B19 site is occupied, it should neighbor a vacant B13 site.

The picture that emerges from these considerations is that in addition to the three vacant B13 sites the eight interstitial boron atoms should be distributed over six B16 and two B19 interstitial sites as homogeneously as possible in accordance with previous work by Jemmis et al.<sup>10</sup> Both occupied B19 sites should lie along the same vector as a vacant B13 site (e.g.,  $2a$  and  $3aB19$  where the  $2a$  and  $3aB13s$  are vacant).

In the discussion of their X-ray data, Slack et al.<sup>7</sup> note that B17 is probably only occupied whenever the neighboring B13E and B13D (in the notation of Slack) are vacant. Indeed, we also observe that a B17 atom can only occur if two neighboring B13 sites are vacant. Moreover, we find that the neighboring B18 site has to be filled simultaneously. This gives support to the suggestion by Slack et al. that B17 and B18 atoms occur in pairs. However (item 4 above), we also see that it is energetically not favorable to occupy any B17 and B18 positions. Slack et al. also postulate that B19 and B20 occur in pairs, and that such pairs only occur when a neighboring B16 is present. Our findings suggest such triples are not energetically favorable.

Slack’s samples were grown from the melt. Defects (complexes) that are unlikely from total energy considerations may be stabilized by entropic effects at elevated temperatures and could be “frozen” into the samples upon cooling. We believe this may explain the partial agreement between our total energy studies and the experimental results.

We now use conclusions listed above to further improve the 106 atom structure. When an atom is moved from the  $\bar{a}B16$  to a  $\bar{b}$  site (106B16b), the energy decreases by 5 meV/B, resulting 23 meV/B below the 105 structure. The gap in the DOS splits into two gaps, one of 0.35 eV at  $E_F$  and one of 1.0 eV at an electron count of 320 (Figure 7). The peak above the Fermi level is analyzed to belong to atoms between the (vacant)  $aB13$  and the (occupied)  $aB16$  sites. We move the atom at the  $aB16$  site to the  $aB19$  site (106B19) since the B19 site is closer to the B13 site than the B16 site. (Two B19 atoms are needed anyway in the 320 atom unit cell, and this is a good check on

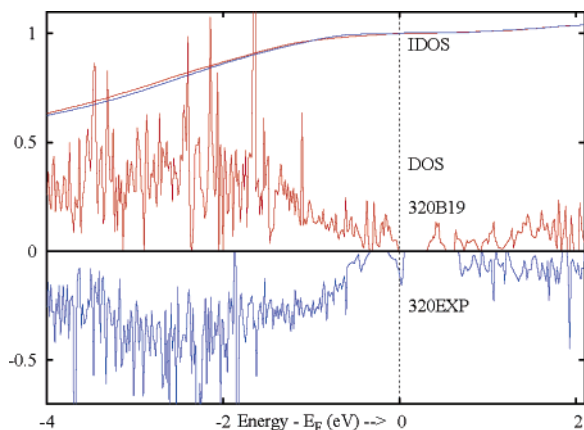


**Figure 8.** Electronic DOS (states/eV/B), energy relative to  $E_F$ , 320 atom hexagonal boron. Both 320B19 (red, upper curve) and 320EXP (blue, lower graph) are shown as well as their IDOS (number of electrons/960). The 320B19 structure is a semiconductor with a gap of 0.35 eV.

their effect.) The energy, however, increases by 2 meV/B, and the gaps in the DOS reunited to one gap of 1.3 eV (Figure 7).

Three final calculations are done with 320 atoms in the unit cell. The first calculation (320B16) has six B16 and two B19 interstitial sites as described above, the second one (320B19) has one B16 less and one B19 more in the same manner, and in the last one (320EXP), we modeled the experimentally observed atomic occupation numbers of the samples of Slack et al.<sup>7</sup> (see Table 2) as well as possible. The precise positioning of interstitial atoms in the calculations are brought together in Table 3. No disorder in the missing B13 positions is considered since the 106 atom cell already gave very good results concerning the total energy and the gap in the DOS. The total energies of the 320 atom structures are not improved over that of the 106B16b structure. The energy of the 320EXP calculation is only 17 meV/B lower than that of the 105 structure. The 320B19d calculation is slightly lower in energy than the 320B16, but slightly higher than that of the 106B16b calculation. The DOSs of 320B19 and 320EXP are displayed in Figure 8. That of 320EXP has a small gap (0.2 eV) just below the Fermi level and a fairly large gap (0.6 eV) just above. It is no semiconductor and therefore cannot represent the experimental structure which has an observed (optical) gap of 1.6 eV.<sup>7</sup> The gap of 320B19 is somewhat smaller (0.35 eV), but it leads to a semiconductor.

Summarizing the study on the interstitial atoms, we found one structure of 106 atoms and one of 320 atoms that are nearly degenerate ( $-23$  meV/B) and show the same band gap (0.35 eV). At first sight, it seems that these cannot represent the experimental structure as the observed gap is no less than 1.6 eV wide.<sup>7</sup> However, thermally stimulated currents, space charge limited currents, and transient photocurrent measurements of the electronic structure of BR boron by Prudenziati et al.<sup>40,41</sup> found that there are (localized) hole traps between 0.23 and 0.36 eV above the valence band. Schmechel and Werheit report gap states in the range from 0.16 to 0.27 eV above the valence band edge.<sup>42,43</sup> These are attributed to probably preferably B13 vacancies or other interstitials. In the DOS of the 106B16b

structure (Figure 7), there is also a localized state above the valence band. It only has contributions from a handful of neighboring atoms, and transitions from the valence band to this state are dipole forbidden (both have only  $p$  character). The optical gap that results is at least 1.4 eV, in good agreement with experimental findings. If two additional electrons (from, e.g., carbon impurities) fill the localized state, it would act as a hole trap instead of an electron trap, as found in experiment. Moreover, the two impurity electrons would also bring the total number of electrons in the unit cell to 320, which would make the agreement with experiment nearly perfect.

We like to stress that although the 106B16b structure is still electron-deficient it exhibits an electronic structure very similar to that of experiment for a specific configuration of a B13 vacancy and two occupied interstitials. This, and it having the lowest energy calculated, strongly suggests that such combinations of defect sites are an essential building block of BR boron. In terms of partial occupancies, this structure has B13 (83%), B16 (33%), B17, and higher (0%). The average occupancy of the samples studied by Slack give B13 (75%), B16 (27%), B17 (7%), B18 (7%), B19 (7%), and B20 (2%). Given that the 106B16b only has three defects (one vacancy and two interstitials), the compositions agree well; indeed, with only three defects, one can hardly approach the experimental compositions better. So there seems ample room within the experimental constraints for 106B16b defect complexes to occur in large quantities. Moreover, Slack's experimental samples may contain "frozen-in" defect structures that are not stable at low temperatures, as noted above. Therefore, perfect agreement with experiment is not to be expected. Of course, many other defect configurations than 106B16b can also occur. Interestingly, Slack et al. do not point out correlations between the occupation of B16 sites, where we do find that a specific configuration of B16 occupations gives a considerable lowering of the total energy. We speculate that such correlations might have been overlooked, as the B16 atoms involved are at a considerable distance apart. It might be an interesting topic for further experimental investigation.

Finally, we also relaxed the lattice parameters (including the cell volume) of the 106B16b structure. This led to a decrease of 0.4% in the volume and marginal changes in the lattice parameters. (Because of the interstitials, the rhombohedral symmetry is broken. As mentioned, changes are very small. The positions and cell parameters are included in the Supporting Information.) We found a bulk modulus of 199 GPa which agrees excellently with the experimental values of 185–210 GPa.<sup>31,44</sup> With the same high kinetic energy cutoffs as that used for the AR structure, the total energy of this structure becomes  $-6.687$  eV/B. We conclude that on the basis of total energies the AR boron is 1 meV/B more stable than the most stable BR structure found.

## 5. Zero Point Energy and Temperature Dependence

Comparing total energies from static electronic structure calculations alone neglects the ZPE of a system. Whereas for heavier elements neglecting the ZPE is reasonable, for the lighter elements, including boron, it is not. Therefore, in the optimized

(40) Prudenziati, M.; Majni, G.; Alberigi Quaranta, A. *J. Phys. Chem. Solids* **1972**, *33*, 245–254.

(41) Prudenziati, M. *J. Less-Common Met.* **1976**, *47*, 113–117.

(42) Schmechel, R.; Werheit, H. *J. Solid State Chem.* **2000**, *154*, 68–74.

(43) Schmechel, R.; Werheit, H. *J. Phys.: Condens. Matter* **1999**, *11*, 6803–6813.

(44) Sanz, D. N.; Loubeyre, P.; Mezouar, M. *Phys. Rev. Lett.* **2002**, *89*, 245501–1–4.

(45) Beckel, C. L.; Yousaf, M.; Fuka, M. Z.; Raja, S. Y.; Lu, N. *Phys. Rev. B* **1991**, *44*, 2535–2553.

**Table 4.**  $\Gamma$ -Point Phonon Frequencies, Symmetry, and Activity [Raman (R) or Infrared (IR)] of  $\alpha$ -Rhombohedral Boron ( $\text{cm}^{-1}$ ), Compared to the Experimental Values: (a) Raman<sup>28,29</sup> and (b) Infrared<sup>45</sup>

mode	active	this work	exp (a)	exp (b)
A <sub>1g</sub>	R	1171	1186	
E <sub>g</sub>	R	1118	1122	
A <sub>2u</sub>	IR	929		
A <sub>1g</sub>	R	921	925	
E <sub>g</sub>	R	870	870	
A <sub>2u</sub>	IR	809		
E <sub>u</sub>	IR	801		806
A <sub>2u</sub>	IR	792		
A <sub>1g</sub>	R	792	793	
A <sub>1u</sub>		787		
E <sub>u</sub>	IR	786		
E <sub>g</sub>	R	773	774	
A <sub>2g</sub>		714		
E <sub>g</sub>	R	708	708	
E <sub>u</sub>	IR	700		705
A <sub>1g</sub>	R	691	692	
E <sub>u</sub>	IR	595		
E <sub>g</sub>	R	582	586	
E <sub>u</sub>	IR	550		548
E <sub>g</sub>	R	521	525	
A <sub>2g</sub>		499		
A <sub>1u</sub>		475		

cells, we calculated the phonon frequencies. The number of atoms in the unit cell differs greatly between AR and BR boron. This causes the band dispersion of the phonon modes to have a large (relative) effect: For AR boron, the difference in ZPE with (using full Brillouin zone integration) and without (using only the  $\Gamma$ -point phonons) band dispersion is 3 meV/B, whereas for BR, it is only 0.2 meV/B. This is mainly caused by the acoustic modes that do not contribute when using only  $\Gamma$ -point phonons. In AR boron, the acoustic modes account for 1/12 of the total number modes, whereas in BR, they account for only 1/106. All phonon contributions reported here are, therefore, integrated over the entire Brillouin zone.

In Table 4, the calculated  $\Gamma$ -point frequencies for AR boron are compared to experimental values. They agree extremely well. By integrating phonon frequencies over the Brillouin zone, we obtain a ZPE of 130 meV/B. This brings the total energy, including ZPE, of AR boron to  $-6.558$  eV/B.

The same procedure was carried out for the most stable 106 structure (106B16b). This gave a ZPE of 126 meV/B, bringing the total energy, including ZPE, of 106B16b BR boron to  $-6.561$  eV/B. For the first time, this gives a BR energy lower than that of AR boron.

The above-reported total energies are, in fact, the Helmholtz free energies at 0 K. At higher temperature, the phonon modes are occupied according to Bose–Einstein statistics. In the harmonic approximation, the Helmholtz free energy is determined by the harmonic lattice vibrations, that is, the phonons, at a volume  $V$ :<sup>46</sup>

$$F(V, T) = U_0(V, T) + \frac{1}{\Omega_{\text{BZ}}} \times \sum_i \int_{\text{BZ}} \left( \frac{\hbar\omega_{\mathbf{q},i}}{2} + \ln[1 - e^{-\hbar\omega_{\mathbf{q},i}/k_{\text{B}}T}] \right) d\mathbf{q}$$

The first term,  $U_0$ , is the total energy of the crystal. The

(46) Wallace, D. C. *Thermodynamics of Crystals*; Wiley: New York, 1972.

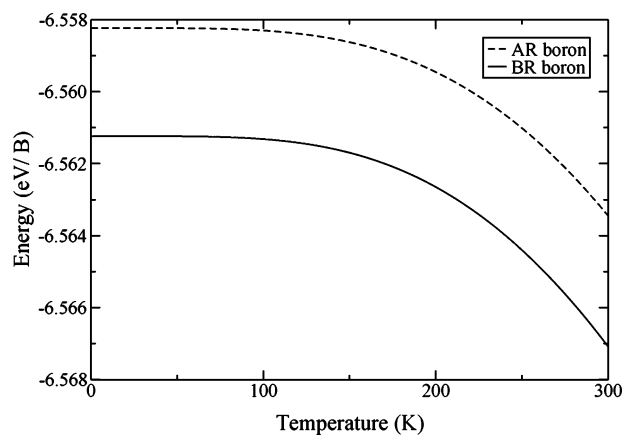


**Figure 9.** Helmholtz free energy (eV/B) at fixed volume, 0 K equilibrium volume, of AR and BR boron as a function of temperature (K).

integration is over the entire Brillouin zone of which  $\Omega_{\text{BZ}}$  denotes the volume. A modified tetrahedron integration method was used.<sup>25</sup> The first term in the integral is the zero point energy, where the  $\omega_{\mathbf{q},i}$  are the phonon angular frequencies at wave vector  $\mathbf{q}$ . The second term in the integral refers to the thermally induced occupation of the various phonon modes.

We fix the volume to the equilibrium value at 0 K and neglect thermal expansion. The bulk moduli of the AR and BR structure are rather similar, so we expect the differences in thermal expansion to be small as well. Since we are only interested in the differences between AR and BR boron, we assume this to be a good approximation.

At finite temperature, there is also a contribution to the free energy from the configurational entropy (CE):

$$\Delta F^{\text{CE}} = -k_{\text{B}}T \ln \left( \sum_i g_i e^{-E_i/k_{\text{B}}T} \right)$$

where  $g_i$  and  $E_i$  are the multiplicities and energies of the various (defect) structures. For BR boron, many defect structures are possible. At a certain temperature and in thermodynamic equilibrium, only those structures significantly contribute whose energies are within  $k_{\text{B}}T$  of the ground state structure. If we only consider the multiplicities of the lowest energy structures (106B16b and 320B19), the  $\Delta F^{\text{CE}}$  is  $-0.6$  meV/B at 300 K. At higher temperatures, the configurational entropy will push down the BR free energy even more. Moreover, well above room temperature, other structures become thermodynamically favorable, and we expect that BR boron is further stabilized. AR boron, on the other hand, has no intrinsic defects at low temperatures and hence no CE contribution. Since the CE effects are small below 300 K, they will not be considered further.

The free energies as a function of temperature are depicted in Figure 9. The difference between AR and BR boron at higher temperatures is marginally larger than that at 0 K. This means that BR boron is the thermodynamically stable allotrope, in correspondence with experimental findings. At temperatures well beyond room temperature, the entropy of the defects will become considerable and thus will stabilize the BR structure even more.

## 6. Conclusions

To summarize, we used first-principles (DFT, GGA) calculations on BR and AR boron to determine the boron ground state

structure. The calculated properties of AR boron, including  $\Gamma$ -point phonon modes, electronic band gap, and bulk modulus, compare very well to experimental values.

The BR 105 atom framework is 26 meV/B higher in energy than AR boron but is stabilized by partial occupations and interstitial atoms. The most stable structure is a 106 atom structure with one B13 site vacant and two atoms added at specific B16 sites. On the basis of this structure, we also constructed a 320 atom unit cell that is nearly as stable. Both are semiconductors with a gap of 0.35 eV. The (optical) gap of the 106 atom structure is (at least) 1.4 eV, which compares favorably with the experimental gap of 1.6 eV.

Relative to AR boron, these structures are still 1 meV/B higher in energy. However, taking the ZPE into account, the BR 106 atom unit cell boron wins at 4 meV with respect to AR boron and becomes the most stable one. Including temperature effects does not change this picture.

Finally, the experimentally determined atomic occupations of BR boron were modeled in a unit cell of 320 atoms. This structure, however, is 6 meV/B higher in energy than the most stable one, and it is no semiconductor.

**Acknowledgment.** The authors wish to thank Dr. T. J. Frankcombe and Dr. C. M. Fang for helpful discussions. This work is part of the research programs of Advanced Chemical Technologies for Sustainability (ACTS) and Stichting voor Fundamenteel Onderzoek der Materie (FOM), financially supported by Nederlandse Organisatie voor Wetenschappelijk Onderzoek (NWO).

**Supporting Information Available:** Unit cell and positions of the 106B16b structure. This material is available free of charge via the Internet at <http://pubs.acs.org>.

JA0631246